

Tropoelastin Massively Associates during Coacervation To Form Quantized Protein Spheres[†]

Adam W. Clarke,[‡] Eva C. Arnspang,[‡] Suzanne M. Mithieux,[‡] Emine Korkmaz,[§] Filip Braet,[§] and Anthony S. Weiss^{*,‡}

School of Molecular and Microbial Biosciences G08 and Australian Key Centre for Microscopy and Microanalysis, University of Sydney, New South Wales 2006, Australia

Received May 21, 2006; Revised Manuscript Received June 21, 2006

ABSTRACT: Tropoelastin, the precursor of elastin, undergoes a rapid monomer to multimer association in an inverse temperature transition. This association culminates in the rapid formation of stable, optically distinct droplets of tropoelastin. Light scattering and microscope measurements reveal that these droplets are 2–6 μm in diameter. Scanning electron microscopy confirms that the droplets are spherical. Three-dimensional confocal image stacks based on the autofluorescence of tropoelastin reveal that droplets are loaded with hydrated tropoelastin. Droplets are viable intermediates in synthetic elastin macroassembly. Dense clusters of aggregated droplets and partially formed fibers develop when droplets are incubated in the presence of a lysyl oxidase. Lysine-reacting chemical and enzyme-assisted cross-linking conditions generate cross-linked beads due to interactions between multiple, surface-exposed lysine ϵ -amino groups. Droplets represent an efficient mechanism for the bolus delivery during elastogenesis of quantized packages of preaccreted tropoelastin.

Elastic fibers impart extensibility and contractibility to connective tissue, which is crucial for physiological function. Elastic fibers are composed primarily of elastin which is a substantially hydrophobic, chemically inert, and insoluble protein mass under normal physiological conditions (1, 2). Greater than 90% of the elastic fiber is composed of elastin. The use of the soluble elastin precursor tropoelastin has permitted in vitro modeling, leading to a greater understanding of the complex interactions that occur in elastic fiber biosynthesis (1, 3–7). Tropoelastin is unusual in that the protein is both soluble and substantially hydrophobic. The hydrophobic amino acids are localized in regions that are punctuated by small hydrophilic domains that include cross-linking domains (8–10). Cross-linking refers to the process of formation of lysine cross-links on tropoelastin, initiated by the enzyme lysyl oxidase, to form elastin (11–13).

Tropoelastin proceeds through a monomer to multimer inverse temperature transition approaching 37 °C in a process termed coacervation (14). This process results in an aggregate mass of protein (15), but it has been assumed that it involves the stepwise addition of tropoelastin monomers. Early studies proposed that coacervation increases order within tropoelastin molecules and aligns them prior to cross-linking during elastogenesis (12). During coacervation, the transformation

of alanine-rich, lysine-containing domains from nascent helices to α -helices promotes the interaction of protein side chains and aligns hydrophobic domains (16–18). The system is reversible, with tropoelastin returning to its previous soluble form when the coacervated solution is cooled (19).

Experiments in which coacervation is inhibited by incubating smooth muscle cells at less than 37 °C demonstrate decreased elastin formation (12). Tropoelastin coacervates, studied by electron microscopy, appear to contain filaments (20) and bundles of fibers (21). These results point to coacervation as an essential step in the formation of elastin.

Early studies on the light scattering properties of coacervating α -elastin provide evidence for the formation of aggregates during coacervation, where at low temperatures (the “off-critical stage”), elastin-derived molecules form small aggregates driven by the poor solubility of its apolar amino acids. In an approach to the critical temperature, solubility decreases and the aggregates increase rapidly where the driving force is an increase in the total entropy of the system (15, 22).

More recent studies establish that an artificial α -elastin coacervate consists of droplets about 1 μm in diameter and accounts for the light scattering that takes place in coacervation. In this system, the slow off-critical self-assembly process is regulated by supplemental electrostatic interactions whereas the fast critical self-assembly process is controlled essentially by hydrophobic interactions. At the critical temperature, collapsing molecular aggregation of α -elastin based on hydrophobic interactions reveals an immediate phase separation associated with large microcoacervate droplets of a broad size distribution (23).

However, there are disadvantages in the use of α -elastin as a descriptor for the coacervation of the natural elastin

[†] A.W.C. received an Australian Postgraduate Award. A.S.W. acknowledges grants from the Australian Research Council and the University of Sydney Vice Chancellor’s Development Fund and Cancer Research Fund.

^{*} To whom correspondence should be addressed. Tel: +61 2 9351 3434. Fax: +61 2 9351 3467. E-mail: a.weiss@mmb.usyd.edu.au.

[‡] School of Molecular and Microbial Biosciences G08, University of Sydney.

[§] Australian Key Centre for Microscopy and Microanalysis, University of Sydney.

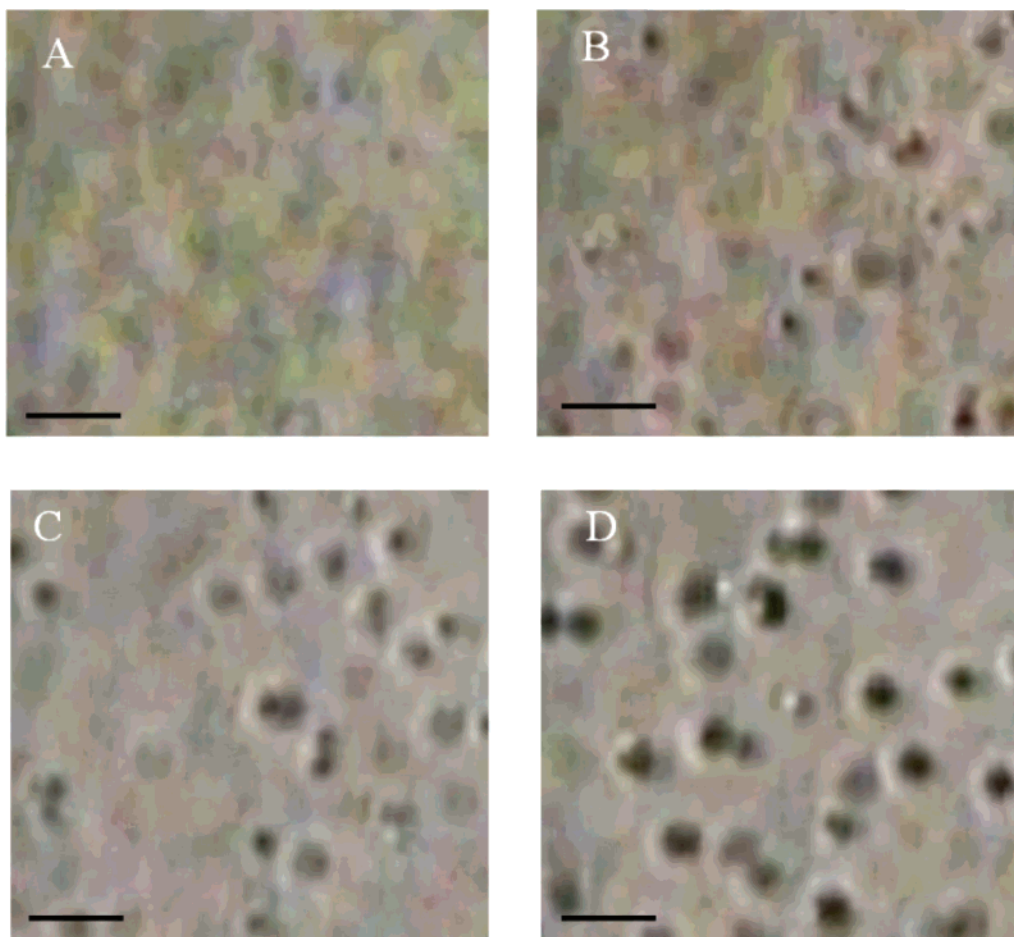


FIGURE 1: Tropoelastin coacervation consists of droplets. Tropoelastin solution was placed between a microscope slide and coverslip. (A) Using an inverted light microscope the process of coacervation was photographed 10 s, (B) 12 s, (C) 14 s, and (D) 16 s after an external heat source was applied. The appearance of droplets can be seen corresponding to coacervation. When formed, these droplets were of uniform size and moved randomly. No interaction was observed between droplets. Scale bar = 10 μm .

precursor, tropoelastin. As α -elastin is obtained from elastin partly hydrolyzed with oxalic acid, it consists primarily of hydrophobic elastin fragments that are heterogeneous and cross-linked, rather than the alternative domain structure observed in natural full-length tropoelastin (24).

In a recent study describing the interactions between tropoelastin and part of fibrillin-1, we found evidence for amassed tropoelastin as a probable assembly intermediate on this part of fibrillin-1 (25). In the current study we explore the physical basis and properties of droplets present in the tropoelastin coacervate. We characterize the sizes and composition of these droplets and detail their ability to interact with and without cross-linking agents. Droplets are an efficient protein-delivery mechanism of tropoelastin packages for in vitro synthetic elastin formation.

MATERIALS AND METHODS

Reagents. Recombinant human tropoelastin was produced as previously described (26). The concentrations of all protein solutions were determined using the BCA assay kit (Pierce). *Pichia pastoris* lysyl oxidase (PPLO)¹ was obtained as a gift from Dr. J. M. Guss (School of Molecular and Microbial Biosciences, University of Sydney) and from Dr. D. M.

Dooley (Department of Chemistry and Biochemistry, Montana State University) (27).

Light Microscopy of Tropoelastin Coacervate. Tropoelastin was prepared in PBS buffer at a concentration of 10 mg/mL. An inverted light microscope (Olympus) with a mounted camera (Sony Electronics) was used to capture images. The 20 μL tropoelastin solution was placed between a microscope slide and coverslip. The temperature of the slide containing tropoelastin was then raised using an external heater until coacervation of tropoelastin occurred. Photographs of the process were captured using the camera. Applied heat was removed, and as the solution cooled, the tropoelastin returned to solution.

Dynamic Light Scattering Experiments of Tropoelastin Coacervate. Determination of the droplet sizes was performed using 10 mg/mL tropoelastin in PBS with a high-performance particle sizer (Malvern Instruments, Malvern, U.K.) with the assistance of Prof. R. G. Gilbert and Dr. R. Mahidasht, Key Centre for Polymer Colloids, University of Sydney. A 2 mL tropoelastin solution was placed into a plastic cuvette and allowed to equilibrate at the required temperature for 5 min. Measurements were then taken over the temperature range 25–37 $^{\circ}\text{C}$.

Phase Contrast Microscopy of Tropoelastin Coacervate Containing BS3. Two microliters of the homobifunctional cross-linker BS3 (60 mg/mL) (28) was added to 20 μL of

¹ Abbreviations: BS3, bis(sulfosuccinimidyl)suberate; PPLO, *Pichia pastoris* lysyl oxidase.

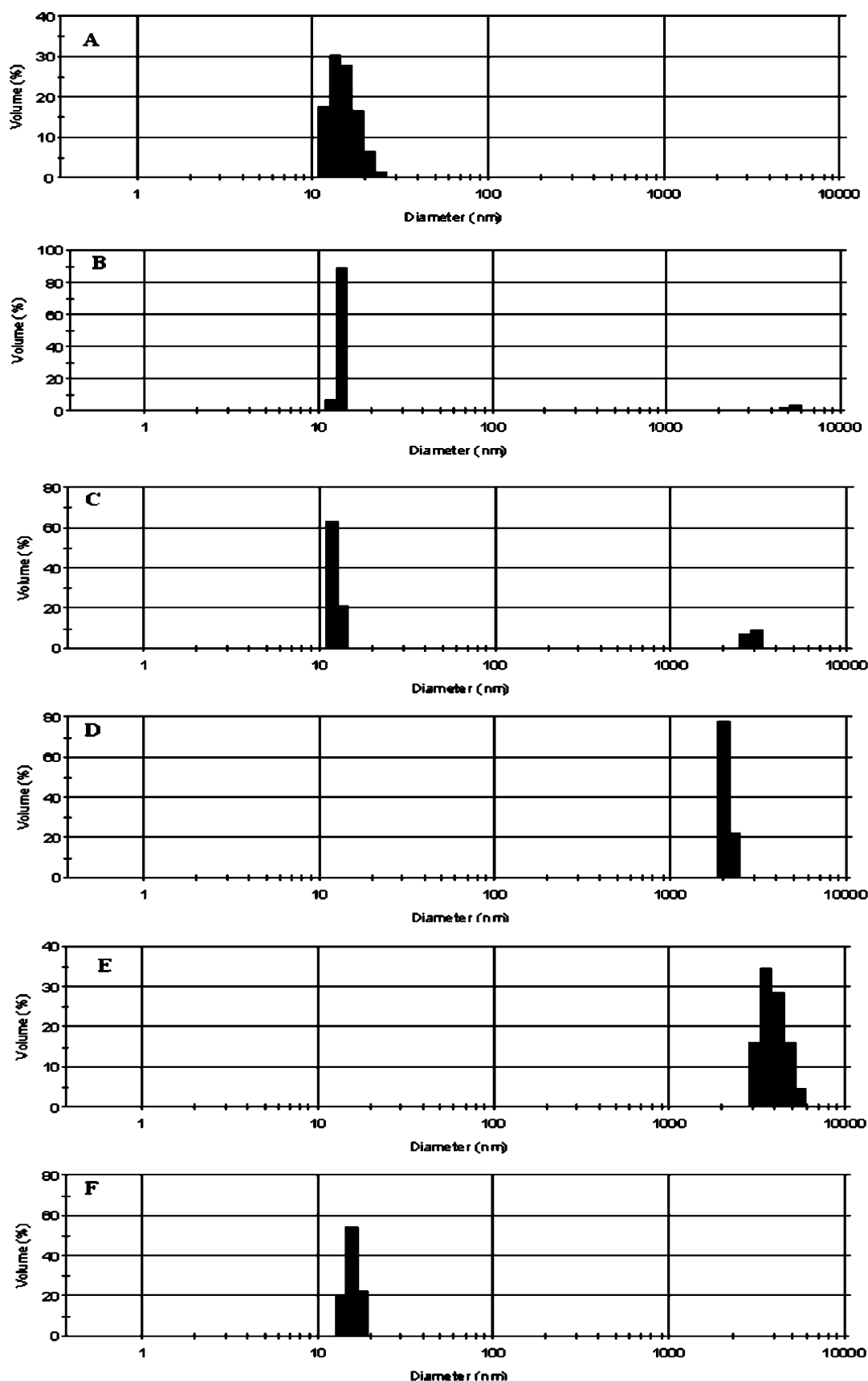


FIGURE 2: Dynamic light scattering measurements of tropoelastin droplets. Dynamic light scattering measurements were performed on 10 mg/mL tropoelastin in PBS. (A) The droplet's size was measured at 29 °C, (B) 31 °C, (C) 32 °C, (D) 33 °C, and (E) 37 °C to display a transition from monomer tropoelastin ~ 15 nm to multimer tropoelastin $\sim 2\text{--}6\text{ }\mu\text{m}$. (F) The reversibility of the system was demonstrated upon cooling to 25 °C at which the monomeric species returns.

tropoelastin in PBS (10 mg/mL). The reaction was performed on the surface of a microscope slide, with BS3 being added

last prior to applying the coverslip. The slide was then placed under a phase contrast microscope (Olympus) with a mounted

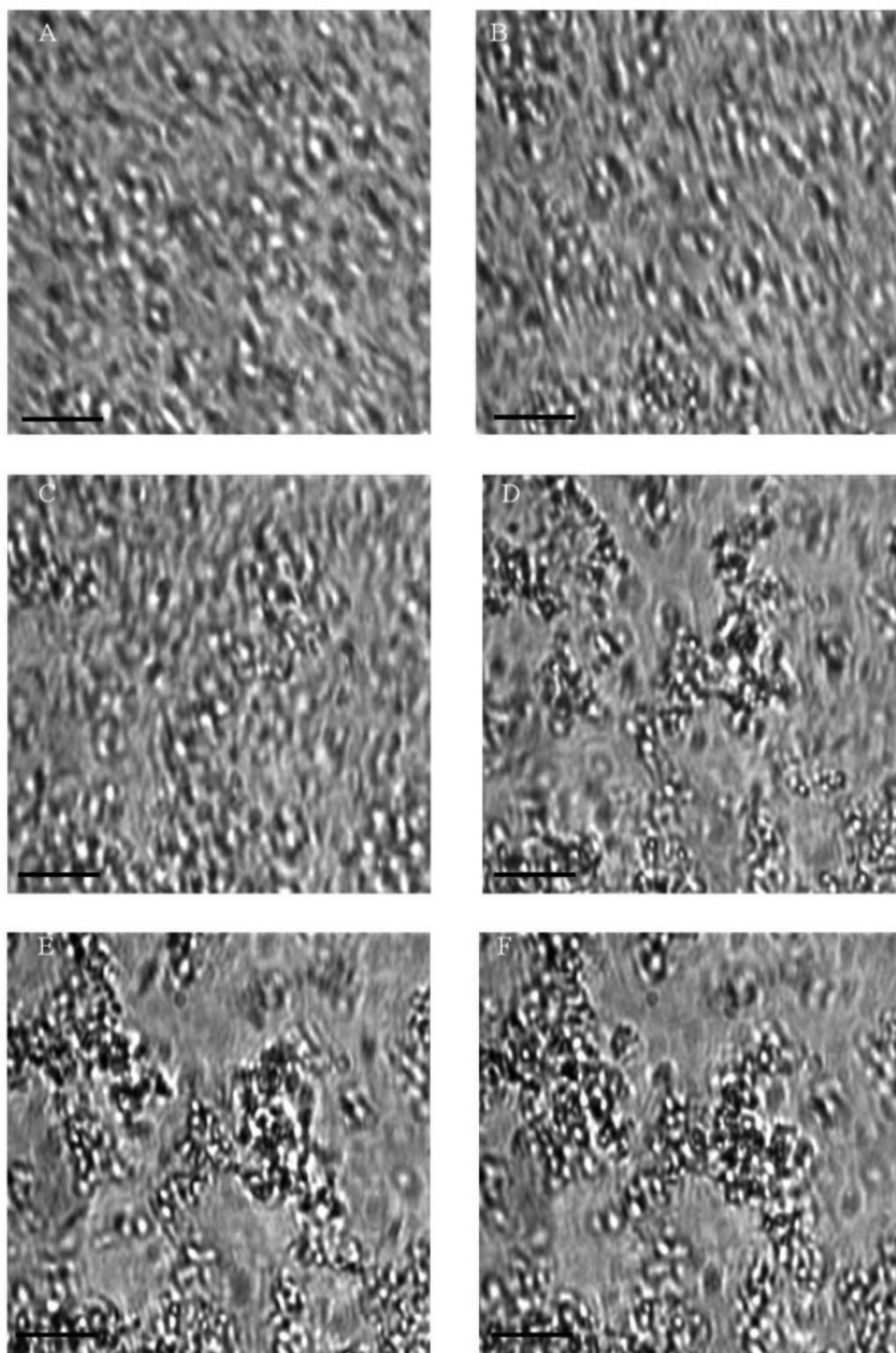


FIGURE 3: Phase contrast microscopy of tropoelastin coacervate containing BS3. Tropoelastin solution was placed on a microscope slide. The homobifunctional cross-linker BS3 was added to the tropoelastin solution, and an external heat source was used to heat the slide. (A) Photographs were taken at 10 s, (B) 15 s, (C) 20 s, (D) 30 s, (E) 45 s, and (F) 1 min after droplet formation first appeared. Scale bar = 20 μm .

camera (Sony Electronics). An external heat source was used to warm the slide until coacervation was observed. The process was captured using the camera. The solution was then allowed to cool to determine the irreversible nature of the cross-linked material.

Confocal Microscopy of Tropoelastin Droplets. Tropoelastin (10 mg/mL) was dissolved in PBS and mounted on 4-well

chamber slides (Lab Tek) and 12-well glass slides (ICN Biomedicals). BS3 was added to cross-link the droplets. The auto-fluorescence of tropoelastin (29) droplets was first measured using images acquired from a Nikon Eclipse E800 microscope using a 100 \times oil, NA = 1.30 objective. A mercury lamp was used to excite tropoelastin with appropriate cutoff filters. Standard FITC, rhodamine, and DAPI filter

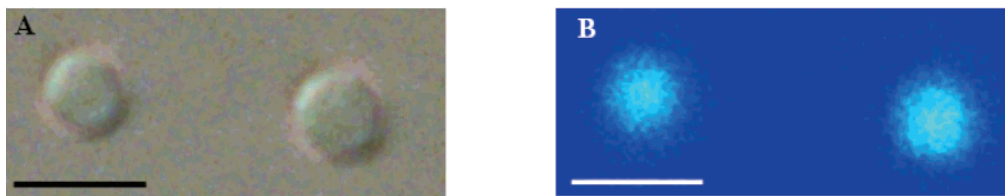


FIGURE 4: Autofluorescence confocal micrographs of tropoelastin droplets fixed with BS3. (A) Tropoelastin coacervate as viewed under a light microscope. (B) Tropoelastin coacervate has intrinsic fluorescence as viewed under a fluorescent microscope. Images were acquired on the Nikon Eclipse TE200 using a 100 \times oil objective (NA = 1.30). Scale bar = 5 μ m.

sets were used for fluorescence imaging. Light microscope micrographs and fluorescent micrographs were obtained using a SensiCam 12 bit cooled imaging CCD camera (PCO Imaging) and the software program CamWare Viewer Gold version 2.2. Further images were acquired on the Nikon Eclipse TE200 using a 100 \times oil objective (NA = 1.30). A solid-state laser 405 nm laser line was used to excite tropoelastin. The filter cube was 450/35, 480 DCLP, and the pinhole diameter was 30 μ m. Standard FITC, rhodamine, and DAPI filter sets were used for fluorescence imaging with a dichroic mirror DM 408/488/561. Single sections and 3D stacks were acquired using high-speed gated detection system and Nikon EZ-C1 software (Nikon). An image stack is typically comprised of a series of 22 images captured at 0.1 μ m intervals. A combination of software (Image J and 3DDoctor) was used to generate surface-rendered three-dimensional images of droplets derived from the image stacks.

Light Microscopy of the Tropoelastin Coacervate Containing BS3. Tropoelastin solution containing cross-linker was prepared as described above but was placed in the well of a 96-well microtiter plate (Greiner). Initially, 20 μ L of tropoelastin solution containing cross-linker was placed in the well and allowed to cross-link as described above. After 10 min images of the resulting cross-linked material were captured using a mounted camera attached to the inverted light microscope. This was repeated using increasing amounts of tropoelastin solution.

Light Microscopy of the Tropoelastin Coacervate Containing *P. pastoris* Lysyl Oxidase. Using small wells on the lid of a 96-well microtiter plate (Greiner), 20 μ L of tropoelastin (5 mg/mL) was mixed with 2 μ L of *P. pastoris* lysyl oxidase (PPLO) (9 mg/mL). A coverslip was applied to seal each well. The assembly was then viewed under an inverted light microscope (Olympus) with a mounted camera (Sony Electronics). Heat was applied until coacervation was reached. Images were captured every minute over a period of 4 h, during which time heat was constantly applied to maintain coacervation. Images were then captured of the resulting biomaterial. Orcein stain was prepared by dissolving 2 g of orcein in 90 mL of hot glacial acetic acid. The solution was cooled and made up to 200 mL with water. Orcein stain was then applied to the biomaterial for 30 min, the excess stain removed, and the sample photographed.

Scanning Electron Microscopy. Samples were rinsed with culture medium and fixed with 2% glutaraldehyde in 0.1 M sodium cacodylate buffer with 0.1 M sucrose for 1 h. Subsequently, samples underwent postfixation with 1% osmium in 0.1 M sodium cacodylate for 1 h and were then dehydrated in ethanol solutions of 70%, 80%, 90%, and 100% (3 times), 10 min each. For drying, the samples were immersed for 3 min in 100% hexamethyldisilazane after the

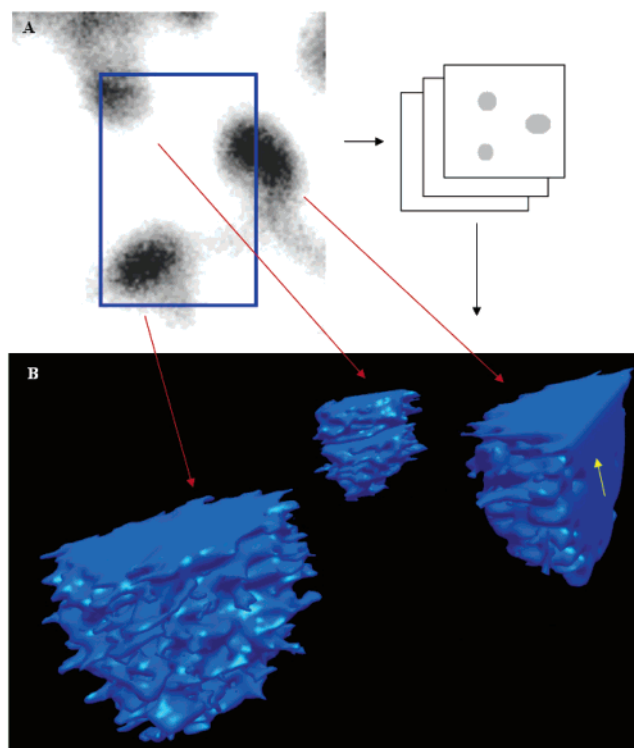


FIGURE 5: Three-dimensional reconstruction of a tropoelastin droplet. (A) Example of a single image used to produce a three-dimensional image stack of a tropoelastin droplet. The blue box refers to the region of the image stack used in the reconstruction. The red arrows refer to droplets that were used in three-dimensional reconstruction. (B) Surface rendered three-dimensional image of tropoelastin droplets fixed using BS3, as derived from an image stack. The droplets consist of a compact mass of tropoelastin (yellow arrow).

100% ethanol step. After HMDS treatment, the samples were transferred to a desiccator for 25 min to avoid water contamination. Next, samples were mounted on stubs, sputter coated with 10 nm gold, and examined with a Philips SEM 505 at 30 kV (30).

RESULTS

Tropoelastin Forms a Droplet Corresponding to Coacervation. Tropoelastin solution was placed between a slide and coverslip and then was gently heated upon which the solution opacified due to coacervation. When viewed under an Olympus inverted light microscope, the coacervate was found to contain droplets (Figure 1) which formed evenly distributed, discrete entities and did not appear to fuse with other droplets.

Particle Size Analysis of Tropoelastin Droplets. At temperatures of up to 29 $^{\circ}$ C, tropoelastin was a monomer of \sim 15 nm in diameter (Figure 2A), in close agreement with

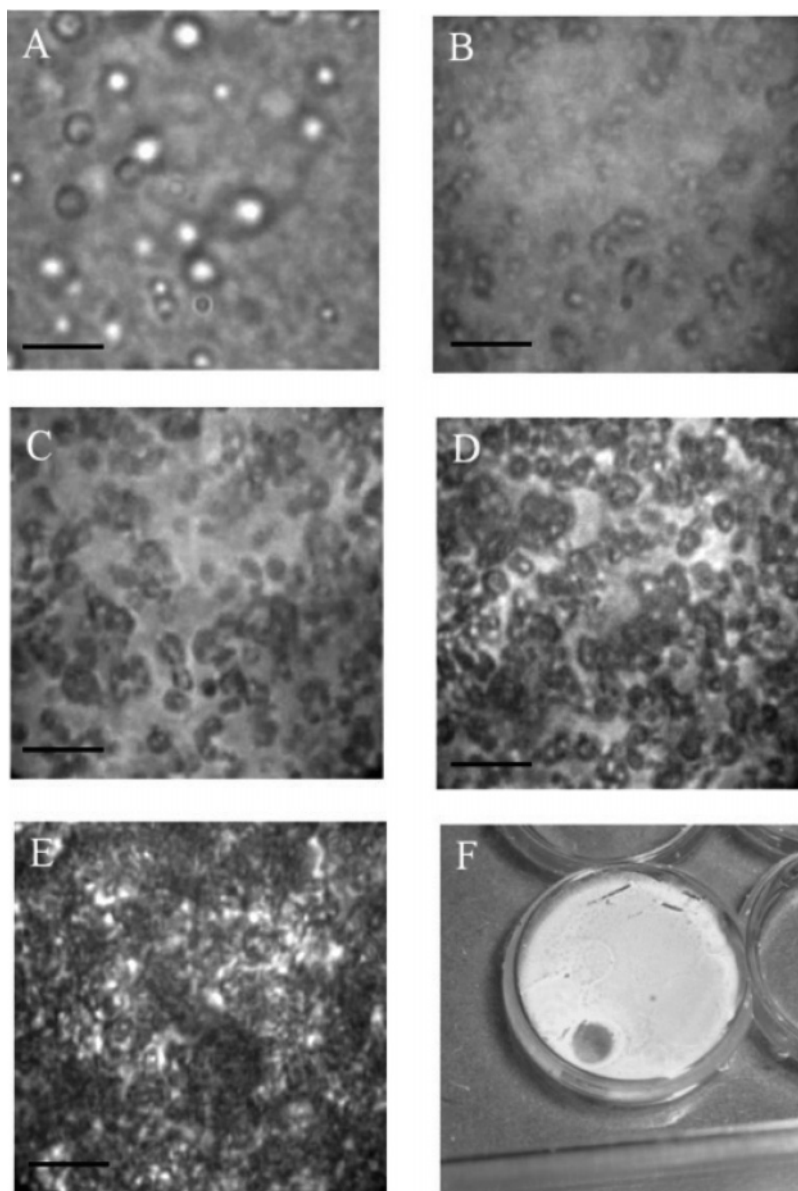


FIGURE 6: Light microscopy of tropoelastin coacervate containing PPLO. Tropoelastin and PPLO were heated until coacervation was reached. (A) Initially coacervation appeared as droplets when viewed using an inverted light microscope. (B) After 30 min the droplets appeared to interact and cluster. (C, D) The clusters of droplets grew in size. (E) Sedimentation of these droplets occurred at 4 h after coacervation. (F) The stacked clusters of droplets formed a dense biomaterial. Scale bar = 20 μm .

previous estimates of a hydrodynamic radius around 6 nm (31). Heating to 31 $^{\circ}\text{C}$ gave droplets of average size $\sim 5 \mu\text{m}$ (Figure 2B). No intermediates were identified, revealing rapid assembly from the monomer. The proportion of droplets relative to monomer tropoelastin increased at 32 $^{\circ}\text{C}$ (Figure 2C). At 33 $^{\circ}\text{C}$ the relative percent volume of droplets to monomer tropoelastin suppressed the detection of the remaining monomer tropoelastin in solution (Figure 2D). At all temperatures, tropoelastin droplets were between 2 and 6 μm (Figure 2E). There was no detectable higher species, confirming that the droplets were a defined size end product. The monomer species returned upon cooling to 25 $^{\circ}\text{C}$, demonstrating the reversibility of this system (Figure 2F).

Tropoelastin Droplets Can Interact in the Presence of a Cross-Linking Reagent. Tropoelastin coacervate was viewed under a phase contrast microscope and did not interact but dissipated upon cooling. In contrast, in the presence of the cross-linking reagent BS3, droplets irreversibly associated

and aggregated into clusters (Figure 3). Upon cooling these aggregates did not dissipate, and droplets remained in an approximately spherical shape. Increasing amounts of tropoelastin solution were mixed with BS3 and resulted in the formation of larger and more dense networks of droplet clusters.

Tropoelastin Droplets Visualized by Confocal Microscopy. Droplets were fixed onto glass surfaces. Confocal microscopy benefited from the intrinsic fluorescence of tropoelastin (Figure 4). An image stack was captured at 0.1 μm intervals through several droplets (Figure 5A) and used to construct surface-rendered three-dimensional images (Figure 5B). The droplets were approximately spherical and contained at least some protein as evidenced by fluorescence within the droplet interior.

Aggregates of PPLO-Mediated Cross-Linked Tropoelastin Droplets Form a Dense Biomaterial. Tropoelastin was heated to coacervate in the presence of PPLO, giving discrete

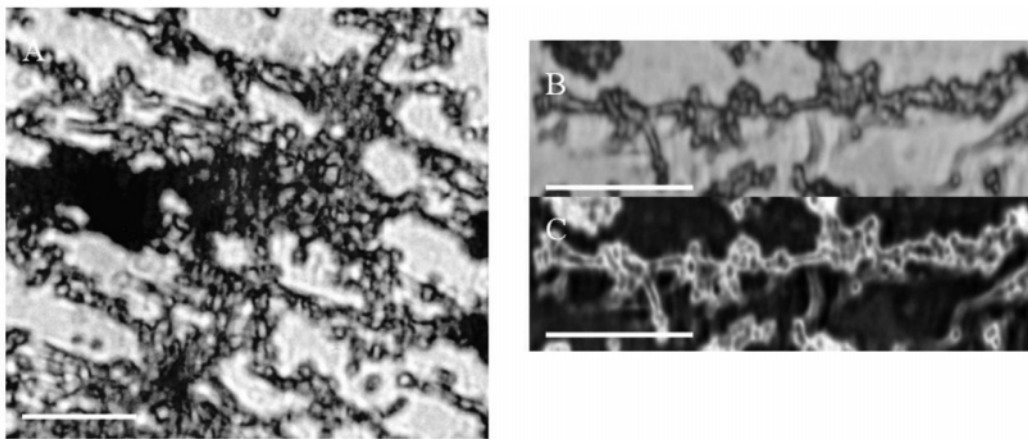


FIGURE 7: Partial fiber formation following PPLO treatment and coacervation of tropoelastin. (A) When stained with orcein, the biomaterial produced also contained remnants of fibers. (B, C) These fibers were interspersed with droplets as seen in the inverted image where the early formation of fibers was achieved through aggregates of coacervated tropoelastin droplets. Scale bar = 30 μm .

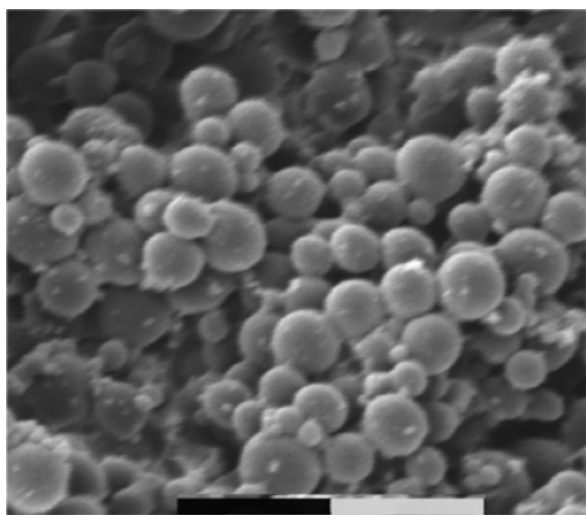


FIGURE 8: High-magnification scanning electron micrograph of tropoelastin, showing the spherical appearance of the tropoelastin droplets. Note that these droplets closely interact and form intricate clusters, confirming the earlier light optical observations. Image data were acquired in eucentric position on a SEM 505 microscope at a magnification of 7500 using 30 kV as accelerating voltage and 6 nm as spot size. Scale bar = 10 μm .

droplets (Figure 6A). Due to amine oxidation and cross-linking, after 30 min aggregates of droplets were observed (Figure 6B). As time progressed, larger structures formed with clustered droplets (Figure 6C,D). At 4 h, the accumulated masses of these large droplet clusters sedimented (Figure 6E), leading to stacked droplet clusters and a relatively dense biomaterial (Figure 6F).

Tropoelastin Droplets Are Able To Form Partial Fibers. Large clusters of aggregated droplets contained fibers (Figure 7A), demonstrating that merged droplets were capable of forming nascent fibers (Figure 7B,C).

Tropoelastin Droplets Are Spherical. Scanning electron microscopy of droplets displayed a consistent population of spheres (Figure 8).

DISCUSSION

In this study we defined the size, content, and interactions of tropoelastin protein assemblies prior to and following cross-linking. The tropoelastin coacervate is a cloudy suspension due to a transition from an ~ 15 nm tropoelastin

monomer to $\sim 2\text{--}6$ μm droplets at 31–32 $^{\circ}\text{C}$ with no detectable intermediates. The volume of tropoelastin droplets was large compared to monomer tropoelastin, so on a scale of percent volume at temperatures above 32 $^{\circ}\text{C}$ no monomer tropoelastin was observed, indicating that the majority of monomeric tropoelastin had been incorporated into the droplets. At 37 $^{\circ}\text{C}$ there were no detectable species larger than about 6 μm , indicating that the droplets did not interact appreciably to form higher order species under these conditions.

It is remarkable that no intermediates were detected in the progression from monomer to droplet. This is consistent with a rapid temperature-dependent association of monomers that is dominated by hydrophobic interactions (16–18).

To test for the presence of hydrophilic regions on the surface of droplets, we used the cross-linking reagent BS3, which reacts with the ϵ -amino group of lysine and forms a synthetic elastin with properties very similar to those of native elastin (28, 32). These lysines are dominantly found in hydrophilic regions of tropoelastin. Interacting droplets were trapped when BS3 was added to a coacervating solution of tropoelastin, leading to large clusters of tropoelastin droplets. This clustering confirms that exposed lysine residues are on the droplet surface and allow for massive cross-linking of multiple droplets.

Each droplet is approximately spherical and contains hydrated tropoelastin, as evidenced by three-dimensional optical sections. To avoid the formation of hollow entities, droplets are likely to grow in an outward manner, as observed in real time imaging of droplet formation, and reach a critical size upon which no further tropoelastin can be incorporated into the droplet.

A layered synthetic elastin biomaterial appeared following the treatment of droplets with the lysyl oxidase PPLO. Droplets interacted, linked, and then settled as clusters and partially formed fibers, revealing that droplets are capable of forming fibers. In vivo it is likely that multiple interactions of tropoelastin droplets with moving cells are needed to define the spatial organization of nascent elastic fibers (38).

This study demonstrates that the tropoelastin coacervate consists of approximately spherical droplets of a fixed diameter and uniformity, with lysine residues on their hydrophilic surfaces. In the presence of lysine cross-linking

reagents, fibrous and clustered aggregates of droplets are produced. This result alters our view of tropoelastin coacervation, in which we now view coacervation as the process of aligning monomer tropoelastin in a droplet arrangement for delivery to a growing elastic fiber.

REFERENCES

- Davidson, J. M., Zhang, M. C., Zoia, O., and Giro, M. G. (1987) *Elastin: structure and biology*, Marcel Dekker, New York.
- Rosenbloom, J. (1987) Elastin: an overview, *Methods Enzymol.* 144, 172–196.
- Mecham, R. P. (1991) Elastin synthesis and fiber assembly, *Ann. N.Y. Acad. Sci.* 624, 137–146.
- Mecham, R. P., Broekelmann, T., Davis, E. C., Gibson, M. A., and Brown-Augsburger, P. (1995) Elastic fibre assembly: macromolecular interactions, *Ciba Found. Symp.* 192, 172–181; discussion 181–184.
- Indik, Z., Abrams, W. R., Kucich, U., Gibson, C. W., Mecham, R. P., and Rosenbloom, J. (1990) Production of recombinant human tropoelastin: characterization and demonstration of immunologic and chemotactic activity, *Arch. Biochem. Biophys.* 280, 80–86.
- Rosenbloom, J., Abrams, W. R., Indik, Z., Yeh, H., Ornstein-Goldstein, N., and Bashir, M. M. (1995) Structure of the elastin gene, *Ciba Found. Symp.* 192, 59–74; discussion 74–80.
- Indik, Z., Yeh, H., Ornstein-Goldstein, N., Kucich, U., Abrams, W., Rosenbloom, J. C., and Rosenbloom, J. (1989) Structure of the elastin gene and alternative splicing of elastin mRNA: implications for human disease, *Am. J. Med. Genet.* 34, 81–90.
- Indik, Z., Yeh, H., Ornstein-Goldstein, N., Sheppard, P., Anderson, N., Rosenbloom, J. C., Peltonen, L., and Rosenbloom, J. (1987) Alternative splicing of human elastin mRNA indicated by sequence analysis of cloned genomic and complementary DNA, *Proc. Natl. Acad. Sci. U.S.A.* 84, 5680–5684.
- Debelle, L., Wei, S. M., Jacob, M. P., Hornebeck, W., and Alix, A. J. (1992) Predictions of the secondary structure and antigenicity of human and bovine tropoelastins, *Eur. Biophys. J.* 21, 321–329.
- Bashir, M. M., Indik, Z., Yeh, H., Ornstein-Goldstein, N., Rosenbloom, J. C., Abrams, W., Fazio, M., Uitto, J., and Rosenbloom, J. (1989) Characterization of the complete human elastin gene. Delineation of unusual features in the 5'-flanking region, *J. Biol. Chem.* 264, 8887–8891.
- Siegel, R. C., Pinnell, S. R., and Martin, G. R. (1970) Cross-linking of collagen and elastin. Properties of lysyl oxidase, *Biochemistry* 9, 4486–4492.
- Narayanan, A. S., Page, R. C., Kuzan, F., and Cooper, C. G. (1978) Elastin cross-linking in vitro. Studies on factors influencing the formation of desmosines by lysyl oxidase action on tropoelastin, *Biochem. J.* 173, 857–862.
- Kagan, H. M., and Sullivan, K. A. (1982) Lysyl oxidase: preparation and role in elastin biosynthesis, *Methods Enzymol.* 82, 637–650.
- Toonkool, P., Jensen, S., Maxwell, A., and Weiss, A. (2001) Hydrophobic domains of human tropoelastin interact in a context-dependent manner, *J. Biol. Chem.* 276, 44575–44580.
- Jamieson, A. M., Downs, C. E., and Walton, A. G. (1972) Studies of elastin coacervation by quasielastic light scattering, *Biochim. Biophys. Acta* 271, 34–47.
- Muiznieks, L. D., Jensen, S. A., and Weiss, A. S. (2003) Structural changes and facilitated association of tropoelastin, *Arch. Biochem. Biophys.* 410, 317–323.
- Rapaka, R. S., and Urry, D. W. (1978) Coacervation of sequential polypeptide models of tropoelastin. Synthesis of H-(Val-Ala-Pro-Gly)_n-Val-OMe and H-(Val-Pro-Gly-Gly)_n-Val-OMe, *Int. J. Pept. Protein Res.* 11, 97–108.
- Tamburro, A. M., Guantieri, V., and Gordini, D. D. (1992) Synthesis and structural studies of a pentapeptide sequence of elastin. Poly (Val-Gly-Gly-Leu-Gly), *J. Biomol. Struct. Dyn.* 10, 441–454.
- Vrhovski, B., Jensen, S., and Weiss, A. S. (1997) Coacervation characteristics of recombinant human tropoelastin, *Eur. J. Biochem.* 250, 92–98.
- Cox, B. A., Starcher, B. C., and Urry, D. W. (1974) Communication: Coacervation of tropoelastin results in fiber formation, *J. Biol. Chem.* 249, 997–998.
- Bressan, G. M., Castellani, I., Giro, M. G., Volpin, D., Fornieri, C., and Pasquali Ronchetti, I. (1983) Banded fibers in tropoelastin coacervates at physiological temperatures, *J. Ultrastruct. Res.* 82, 335–340.
- Jamieson, A. M., Simic-Glavaski, B., Tansey, K., and Walton, A. G. (1976) Studies of elastin coacervation by quasielastic light scattering, *Faraday Discuss. Chem. Soc.*, 194–204.
- Kaibara, K., Watanabe, T., and Miyakawa, K. (2000) Characterizations of critical processes in liquid-liquid-phase separation of the elastomeric protein-water system: microscopic observations and light scattering measurements, *Biopolymers* 53, 369–379.
- Vrhovski, B., and Weiss, A. S. (1998) Biochemistry of tropoelastin, *Eur. J. Biochem.* 258, 1–18.
- Clarke, A. W., Wise, S. G., Cain, S. A., Kielty, C. M., and Weiss, A. S. (2005) Coacervation is promoted by molecular interactions between the PF2 segment of fibrillin-1 and the domain 4 region of tropoelastin, *Biochemistry* 44, 10271–10281.
- Martin, S. L., Vrhovski, B., and Weiss, A. S. (1995) Total synthesis and expression in *Escherichia coli* of a gene encoding human tropoelastin, *Gene* 154, 159–166.
- Mithieux, S. M., Wise, S. G., Raftery, M. J., Starcher, B., and Weiss, A. S. (2005) A model two-component system for studying the architecture of elastin assembly in vitro, *J. Struct. Biol.* 149, 282–289.
- Wise, S. G., Mithieux, S. M., Raftery, M. J., and Weiss, A. S. (2005) Specificity in the coacervation of tropoelastin: solvent exposed lysines, *J. Struct. Biol.* 149, 273–281.
- Mithieux, S. M., Rasko, J. E., and Weiss, A. S. (2004) Synthetic elastin hydrogels derived from massive elastic assemblies of self-organized human protein monomers, *Biomaterials* 25, 4921–4927.
- Braet, F., de Zanger, R., and Wisse, E. (1997) Drying cells for SEM, AFM and TEM by hexamethyldisilazane: a study on hepatic endothelial cells, *J. Microsc.* 186, 84–87.
- Toonkool, P., Regan, D. G., Kuchel, P. W., Morris, M. B., and Weiss, A. S. (2001) Thermodynamic and hydrodynamic properties of human tropoelastin. Analytical ultracentrifuge and pulsed field-gradient spin-echo NMR studies, *J. Biol. Chem.* 276, 28042–28050.
- Mithieux, S. M., Rasko, J. E. J., and Weiss, A. S. (2004) Synthetic elastin hydrogels derived from massive elastic assemblies of self-organized human protein monomers, *Biomaterials* 25, 4921–4927.
- Nakamura, T., Lozano, P. R., Ikeda, Y., Iwanaga, Y., Hinek, A., Minamisawa, S., Cheng, C. F., Kobuke, K., Dalton, N., Takada, Y., Tashiro, K., Ross Jr, J., Honjo, T., and Chien, K. R. (2002) Fibulin-5/DANCE is essential for elastogenesis in vivo, *Nature* 415, 171–175.
- Yanagisawa, H., Davis, E. C., Starcher, B. C., Ouchi, T., Yanagisawa, M., Richardson, J. A., and Olson, E. N. (2002) Fibulin-5 is an elastin-binding protein essential for elastic fibre development in vivo, *Nature* 415, 168–171.
- Clarke, A. W., and Weiss, A. S. (2004) Microfibril-associated glycoprotein-1 binding to tropoelastin: multiple binding sites and the role of divalent cations, *Eur. J. Biochem.* 271, 3085–3090.
- Rock, M. J., Cain, S. A., Freeman, L. J., Morgan, A., Mellody, K., Marson, A., Shuttleworth, C. A., Weiss, A. S., and Kielty, C. M. (2004) Molecular basis of elastic fiber formation. Critical interactions and a tropoelastin-fibrillin-1 cross-link, *J. Biol. Chem.* 279, 23748–23758.
- Lauffer, M. A. (1975) *Entropy-Driven Processes in Biology: Polymerisation of Tobacco Mosaic Virus Protein and Similar Reactions*, Chapman & Hall Ltd., London.
- Czirok, A., Zach, J., Kozel, B. A., Mecham, R. P., Davis, E. C., and Rongish, B. J. (2006) Elastic fiber macro-assembly is a hierarchical, cell motion-mediated process, *J. Cell. Physiol.* 207, 97–106.